Extending the Vibrational Lifetime of Azides with Heavy Atoms

Farzaneh Chalyavi, Andrew J. Schmitz, Natalie R. Fetto, Matthew J. Tucker,* Scott H. Brewer,* and Edward E. Fenlon*

SUPPORTING INFORMATION

Table of Contents

EXPERIMENTAL METHODS

Synthetic Procedures.

Reagents were obtained from Sigma-Aldrich, Oakwood, or Acros and were used without further purification. Triple-labeled sodium azide ($Na^{15}N_3$) was purchased from Icon Isotopes. NMR spectra were acquired in $CDCl_3$ solution with a Varian INOVA multinuclear Fourier transform NMR spectrometer at the following frequencies: ^1H (498.9 MHz), ^{29}Si (99.1 MHz), and ^{119}Sn (186.0 MHz). Chemical shifts are reported in parts per million (ppm). ^1H and ^{29}Si NMR spectra were referenced to internal TMS ($SiMe_4$ = 0.0 ppm). ^{119}Sn NMR spectra were referenced to tetra-*n*-propyltin at -16.8 ppm (equivalent to $SnMe_4$ = 0.0 ppm). IR spectra for characterization purposes were obtained as ATR spectra of a thin film and the absorptions are reported in cm^{-1} with relative intensities (vs = very strong, s = strong, m = medium, w = weak).

Triphenylmethyl Azide.[1] **CAUTION:** HN_3 generated in situ during this procedure. Be sure to conduct in a well-ventilated fume hood. To a mixture of sodium azide (1.00 g, 15.4 mmol), H_2O (2 mL), and $CHCl_3$ (4 mL) was added a solution of trityl alcohol (1.00 g, 3.8 mmol) in $CHCl_3$. The mixture was stirred in an ice-water bath while concentrated H_2SO_4 (1.0 mL) was added dropwise from an addition funnel. The mixture was then stirred at ice-bath temperature for 1.5 h. Additional ice was added to the cooling bath and the reaction was basified to pH >12 using 6 M HCl. Water and CH_2Cl_2 were added and the organic layer was washed with water and brine. The organic layer was dried (Na_2SO_4) and then concentrated under reduced pressure. The product was recrystallized by dissolving in room temperature hexane and then putting the solution in a -80 °C freezer to yield 821 mg (75%) of the title compound as a white solid. mp = 61.7-63.4 °C (Lit.[1] mp = 64-65 °C); IR 3332 (w), 3060 (m), 2493 (w), 2195 (w), 2094.8 (vs), 1961 (w), 1882 (w), 1812 (w), 1595 (m), 1491 (s), 1446 (s), 1390 (w), 1323 (m), 1252 (s), 1156 (m), 1085 (m), 1036 (m), 1003 (m), 943 (m), 898 (s), 850 (w), 757 (vs), 697 (vs) cm^{-1}.

Triple-labeled Triphenylmethyl Azide. CAUTION: $H^{15}N_3$ generated in situ during this procedure. Be sure to conduct in a well-ventilated fume hood. This compound was prepared following the procedure for the unlabeled compound: $Na^{15}N_3$ (103 mg, 1.5 mmol), Ph_3COH (98 mg, 0.38 mmol) yielded 79 mg (73%) of the title compound as a white solid/oil. The labeled compound was not recrystallized. IR 3481 (w), 3064 (m), 3034 (m), 2031.4 (vs), 1599 (m), 1491 (s), 1446 (s), 1327 (m), 1215 (s), 1156 (m), 1085 (w), 1010 (m), 939 (m), 895 (m), 760 (s), 701 (vs) cm^{-1}.

Triphenylsilyl Azide.[2] To a flame-dried flask was added triphenylsilyl chloride (490 mg, 1.66 mmol), sodium azide (149 mg, 2.29 mmol; dried overnight in a 109 °C oven), and anhydrous THF (8 mL). The reaction mixture was heated at reflux for 20 h. The reaction mixture was cooled and the supernate was filtered into a dry flask and the solvent was removed under reduced pressure to give 485 mg (97%) of the title compound as a clear, colorless oil that crystallized to a white solid upon standing. mp = 76.3-76.9 °C (Lit.[2] mp = 79 °C); IR 3683 (w), 3071 (w), 2139.5 (vs), 1968 (w), 1893 (w), 1830 (w), 1778 (w), 1670 (w), 1588 (m), 1487 (m), 1431 (s), 1379 (m), 1316 (s), 1264 (m), 1189 (m), 1118 (vs), 1029 (m), 999 (m), 835 (m), 805 (m), 746 (m), 701 (vs) cm^{-1}; ^{1}H NMR δ 7.68-7.28 (m, 15H) ppm; ^{29}Si NMR δ -13.60 ppm.

Triple-labeled Triphenylsilyl Azide. This compound was prepared following the procedure for the unlabeled compound: $Na^{15}N_3$ (82 mg, 1.2 mmol), Ph_3SiCl (301 mg, 1.0 mmol) yielded 305 mg (98%) of the title compound as a white solid. IR 3071 (w), 3027 (w), 2967 (w), 2068.7 (vs), 1964 (w), 1894 (w), 1826 (w), 1774 (w), 1662 (w), 1592 (m), 1487 (m), 1431 (s), 1364 (w), 1259 (s), 1189 (m), 1118 (vs), 1029 (m), 921 (m), 801 (m), 742 (m), 697 (vs) cm^{-1}.

Triphenyltin Azide.[3] A solution of triphenyltin chloride (1.0 g, 2.6 mmol) in diethyl ether (25 mL) was shaken with a solution of sodium azide (227 mg, 3.5 mmol) in water (40 mL) for 10 min. The organic layer was separated and the aqueous layer was extracted with diethyl ether (1×25 mL). The combined organic layers were washed with brine, dried (Na_2SO_4), and concentrated under reduced pressure to give 893 mg (88%) of the title compound as a white solid. mp = 108.7-110.6 °C (Lit.[3]) mp = 115 °C); IR 3067 (m), 3049 (m), 2065 (vs), 1961 (w), 1882 (w), 1819 (w), 1580 (w), 1484 (m), 1431 (s), 1334 (m), 1263 (w), 1193 (w), 1077 (s), 1021 (m), 995 (m), 726 (vs), 697 (vs) cm^{-1}; ^{119}Sn NMR δ -89.18 ppm.

Triple-labeled Triphenyltin Azide. This compound was prepared following the procedure for the unlabeled compound: $Na^{15}N_3$ (44 mg, 0.65 mmol), Ph_3SnCl (205 mg, 0.53 mmol) yielded 155 mg (74%) of the title compound as a white solid. IR 3068 (m), 3049 (m), 1997.9 (vs), 1886 (w), 1819 (w), 1580 (w), 1484 (m), 1431 (s), 1334 (m), 1305 (m), 1233 (m), 1159 (w), 1189 (w), 1077 (s), 1024 (m), 999 (m), 913 (w), 854 (w), 727 vs), 693 (vs) cm^{-1}.

Tributyltin Azide.[4, 5] To a solution of tributyltin chloride (949 mg, 2.9 mmol) in diethyl ether (3 mL) was added a solution of sodium azide (253 mg, 3.9 mmol) in water (3 mL). The biphasic mixture was stirred vigorously at ambient temperature overnight. The mixture was diluted with diethyl ether and water and the organic layer was collected. The aqueous layer was extracted with diethyl ether (2×) and the combined organic layers were dried (Na_2SO_4), and concentrated under reduced pressure to give 852 mg (88%) of the title compound as a clear colorless liquid. IR 2960 (s), 2922 (s), 2855 (m), 2064.9 (vs), 1461 (m), 1416 (w), 1379 (w), 1342 (m), 1275 (w), 1182 (w), 1077 (m), 1025 (w), 982 (w), 876 (m), 772 (w), 671 (s) cm^{-1} ; ^{119}Sn NMR δ 110.78 ppm.

Triple-labeled Tributyltin Azide. This compound was prepared following the procedure for the unlabeled compound: $Na^{15}N_3$ (50.6 mg, 0.74 mmol), Bu_3SnCl (163 µL, 0.53 mmol) yielded 168 mg (84%) of the title compound as a clear colorless liquid. IR 2960 (s), 2922 (s), 2855 (m), 1994.1 (vs), 1461 (m), 1416 (w), 1379 (w), 1293 (w), 1252 (w), 1182 (w), 1077 (w), 1025 (w), 962 (w), 880 (w), 697 (w) cm^{-1}.

Linear IR Measurements.

Equilibrium FTIR absorbance spectra were recorded on a Bruker Vertex 70 FTIR spectrometer equipped with a globar source, KBr beamsplitter, and a liquid nitrogen cooled mercury cadmium telluride (MCT) detector. The spectra were measured using a temperature-controlled, two-compartment transmission cell consisting of calcium fluoride (CaF_2) windows with a path length of approximately 55 µm at a resolution of 1 cm^{-1}. The absorbance spectra were the result of 128 scans and the temperature was measured using an embedded thermocouple in the cell. The spectra were intensity normalized and baseline corrected.

Transient Absorption Measurements.

Vibrational population relaxation was measured via an infrared pump-probe experiment. A CaF_2 sample cell with path length of 50 μm contained concentrations of ~20 mM of the group 14 atom azide compounds in THF. Fourier-transformed limited pulses of approximately 80 fs in bandwidth were used with center frequencies set at each sample's respective excitation energy. The mid-IR is split with a ZnSe beamsplitter to generate pump and probe pules of 1.5 μJ and 1 μJ, respectively. The beam size of the probe pulse is ~75% of the pump with both having the same polarization. To reduce scattering every other pump pulse is chopped and subtracted with the program. The pump and probe pulses were aligned with a 200 μm pin hole and then sodium azide in D_2O was utilized to achieve maximum spatial and temporal overlap. Following that the wavelength was changed to match the corresponding excitation energy and each sample was spatially aligned (although minimum adjustment was needed) at T = 0 to ensure maximum overlap. As each sample possesses a significant transition dipole, which is advantageous compared to nitriles, spatial alignment was possible for each individual sample. The transmitted probe pulse was routed to a parabola to focus into a monochromator with a liquid nitrogen cooled 64 array mercury-cadmium-telluride (InfraRed Associates, Stuart, FL) and a grating of 75 lines per mm.

Due to the time sensitivity of these samples, four scans were performed at 900 shots up to 105 ps, where 5 ps prior to T = 0 were collected, representing the free induction decay and to discount the possibility of any thermal effects. The raw data was collected with a time step of 10 fs over a total time of 105 ps. The pump probe spectrum was collected over the whole time and no signals were observed due to thermal effects (see Figure S4-S9).

The kinetic traces were determined by taking the maximum intensity of the ground state bleach ($\upsilon = 0 \rightarrow \upsilon = 1$ transition) and plotting it as a function of the total time. The raw data was further processed using a running average by binning every 66 points resulting in the plot of the averaged data with 660 fs step over the whole time range. After binning the data, the averaged kinetic traces were fit to a bi-exponential function of the $S(t) = Ae^{-t/T} + Be^{-t/T`}$, where T and T` are the vibrational lifetimes and A and B are the corresponding amplitudes. Since no significant contributions are expected from THF, an exponential decay is sufficient.[6]

Fast Component Analysis.

To more accurately capture the fast component of the vibrational lifetime, the raw data was reprocessed using a running averaging by binning every 19 points resulting in a plot of average data with 190 fs steps to increase the number of points. Using a truncated window, the averaged data was fit to a single exponential fit of y(t)=Aexp(-t/T) where A is the amplitude and T is the vibrational lifetime and shown as the insets in Figure 3 of the manuscript. The following are the results of those fits to the fast components:

Ph_3CN_3: 2.1±0.2 ps
$Ph_3C^{15}N_3$: 2.0±0.1 ps
Ph_3SiN_3: 1.8±0.1 ps
$Ph_3Si^{15}N_3$: 2.4±0.1 ps
Ph_3SnN_3: 4.8±0.1 ps
$Ph_3Sn^{15}N_3$: 6.4±0.1 ps
Bu_3SnN_3: 6.5±0.2 ps
$Bu_3Sn^{15}N_3$: 6.8±0.2 ps

The short components measured here are similar to that found with the bi-exponential decay.

2D IR Measurements.

Heterodyned spectral interferometry was utilized for obtaining the 2D IR spectra. Fourier-transform limited 80 fs pulses with a central wavelength ranging from 4700 - 5000 nm were employed in the 2D IR experiments. Three ~1 μJ laser pulses with wave vectors k_1, k_2 , and k_3 were incident to the sample generating a signal in the direction $k_s = -k_1 + k_2 + k_3$ with the ordering 123 (rephasing) and 213 (nonrephasing). To obtain absorptive spectra, the rephasing and nonrephasing 2D frequency spectra were properly phased and combined. To observe any changes in the spectral characteristics, the waiting time, T, between the second and third pulse was varied from 0 to 101 ps. After appropriate Fourier transforms along the coherence, τ, and detection, t, axes, the 2D IR spectra were plotted as ω_τ vs ω_t. The vibrational relaxation time, T_{10}, for the two main transitions were estimated from the signal strength of the diagonal peak within the 2D IR at different T values.[7]

The 2D IR spectra of $Ph_3C^{15}N_3$, Ph_3CN_3, and $Ph_3Sn^{15}N_3$ in THF at 1/e of the vibrational lifetime determined from pump-probe measurements, were collected (Figure S1 - S3). The azido- transition is detected at later waiting times. However, there are some distortion associated with the noise present at the later time (T>100ps) due to lower signal strength that can affect the inhomogenous broadening. In some cases, the 2D IR spectrum at later times starts to become slightly distorted because of the signal to noise ratio.

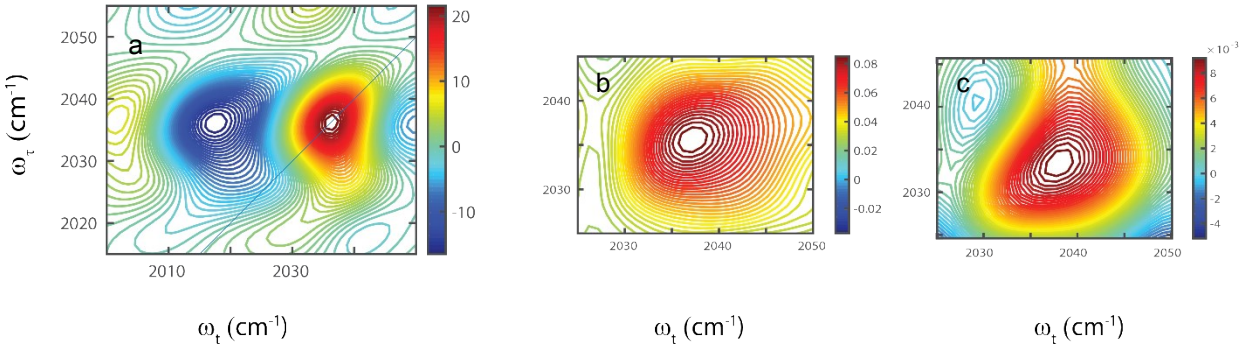

Figure S1. 2D IR spectra of $Ph_3C^{15}N_3$ at waiting times of 1 ps (a), 61 ps (b), and 101 ps (c).

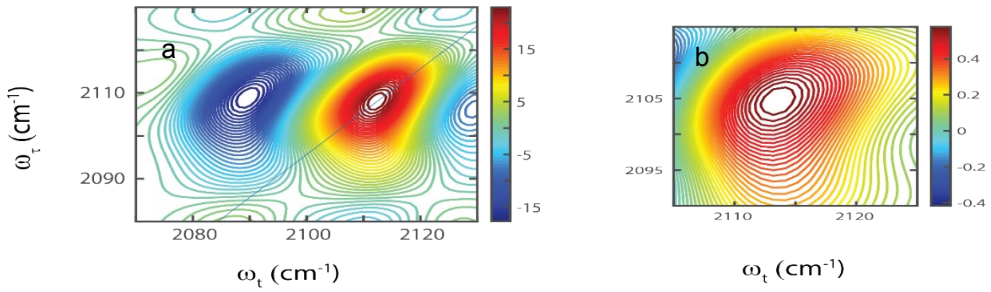

Figure S2. 2D IR spectra of Ph_3CN_3 at T = 500 fs (a) and T = 18.5 ps (b).

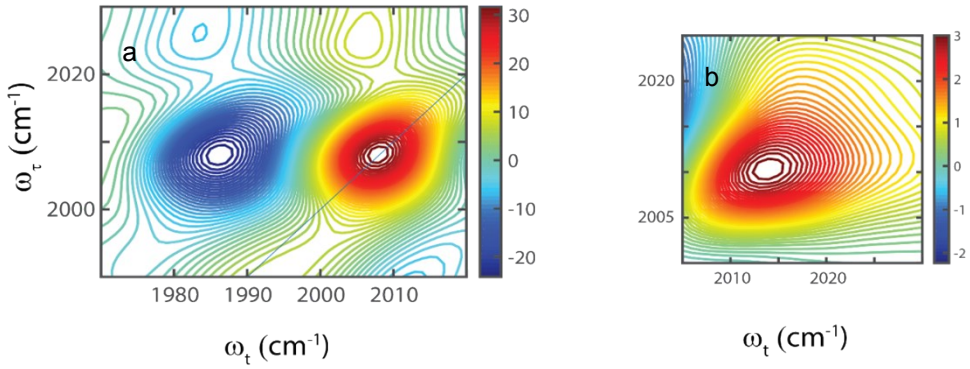

Figure S3. 2D IR spectra of $Ph_3Sn^{15}N_3$ at T = 2 ps (a) and T = 20 ps (b).

Pump Probe Spectra.

The positive peak in pump-probe measurements (Figure S4 – S9) is due to 0 → 1 transition ground state adsorption and stimulated emission. The negative peak is anharmonically red-shifted and representing the excited state absorption for 1→ 2 transition. Pump-probe data at 4 different times, T = 0, 2, 10 and 20 ps has been shown for all the molecules that reveal vibrational relaxation over the waiting time, T.

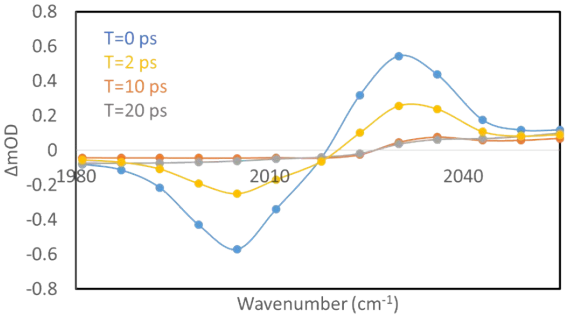

Figure S4. Pump-probe measurement for $Ph_3C^{15}N_3$ at T = 0, 2, 10, and 20 ps.

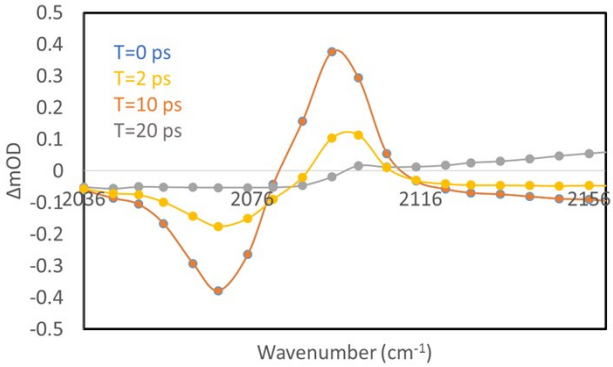

Figure S5. Pump-probe measurement for Ph_3CN_3 at T = 0, 2, 10, and 20 ps.

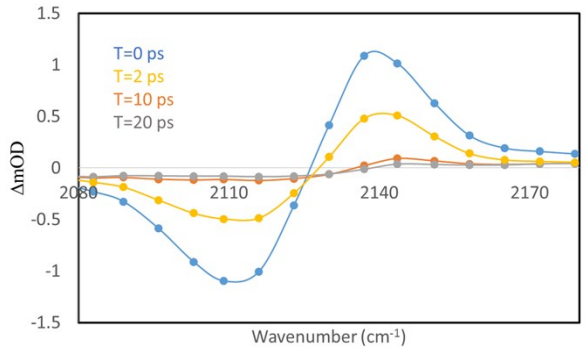

Figure S6. Pump-probe measurement for Ph_3SiN_3 at T = 0, 2, 10, and 20 ps.

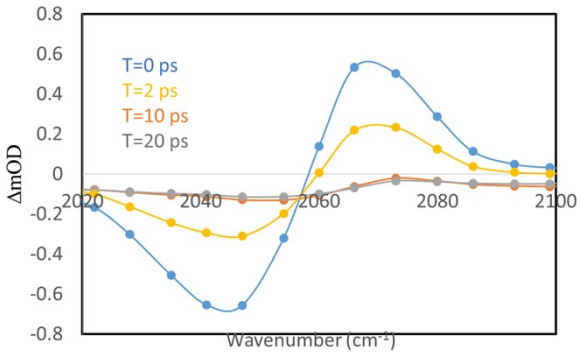

Figure S7. Pump-probe measurement for $Ph_3Si^{15}N_3$ at T = 0, 2, 10,and 20 ps.

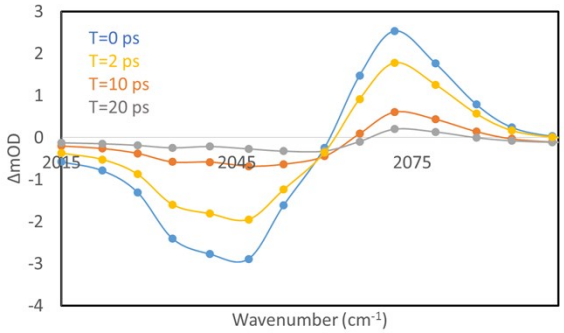

Figure S8. Pump-probe measurement for Ph_3SnN_3 at T = 0, 2, 10, and 20 ps.

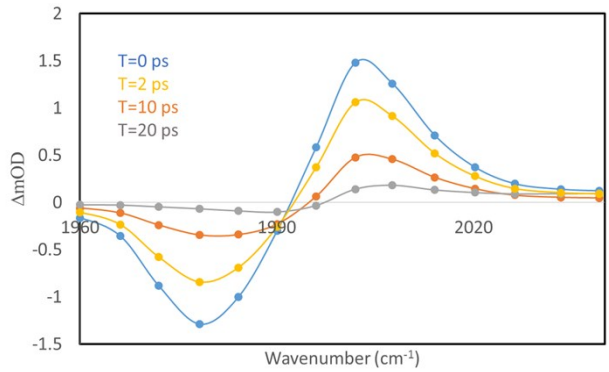

Figure S9. Pump-probe measurement for $Ph_3Sn^{15}N_3$ at T = 0, 2, 10, and 20 ps.

Density Functional Theory (DFT) Calculations.

The DFT calculations were performed on Ph_3EN_3 and $Ph_3E^{15}N_3$ where E is C, Si, or Sn in addition to Bu_3SnN_3 and $Bu_3Sn^{15}N_3$ using the quantum chemical software package Gaussian 16.[8] The gas phase geometry optimizations and vibrational analyses were performed using the B3LYP density functional[9, 10] and the 6-311++G(3df,3pd) basis set[11, 12] for Ph_3EN_3 and $Ph_3E^{15}N_3$ where E is C, Si, and the LANL2DZ basis set[13] for Ph_3SnN_3, $Ph_3Sn^{15}N_3$, Bu_3SnN_3, and $Bu_3Sn^{15}N_3$. Scaling factors of 0.9679 and 0.961 were utilized for the vibrational frequencies calculated using the 6-311++G(3df,3pd) and LANL2DZ basis sets, respectively. The structures were constructed and the vibrational modes visualized using the graphical user interface GaussView 6.

Ph_3SnN_3 band structure analysis.

As shown below, the infrared spectrum of Ph_3SnN_3 in THF were measured at high concentration (~134 mM) and low concentration (~52 mM) indicating complexation was not likely responsible for the band structure (see Figure S10). Second, the temperature dependence of the infrared spectrum was measured over a range of 22 to 60 °C (see Figure S11). As the temperature is increased, the ratio of the larger peak to the shoulder decreases. Overall, these results suggest that the band structure is likely due to some intermolecular interactions with solvent.

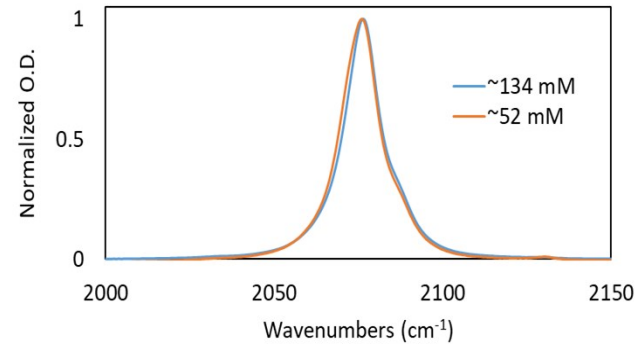

Figure S10. Normalized FTIR spectra of Ph_3SnN_3 in THF at different concentrations of 134mM (blue) and 52mM (orange)

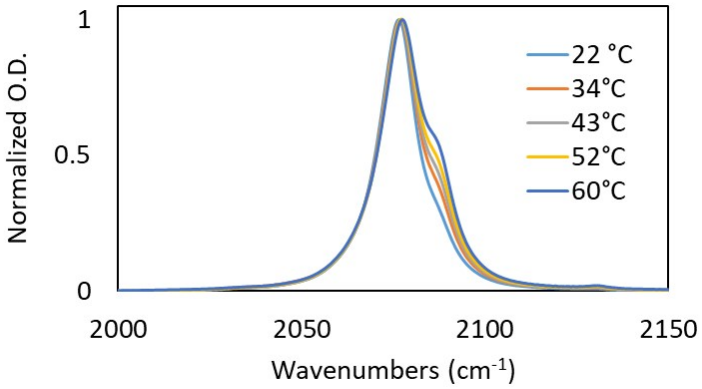

Figure S11. Normalized FTIR spectra of Ph_3SnN_3 in THF at different temperatures 22-60°C

Reorientation components to the vibrational lifetimes.

The possible contributions of reorientation components to the vibrational lifetimes measured via polarized pump-probe measurements, with the pump beam set to the magic angle (~57.4°), were performed on the C centered compound (Figure S12). The magic angle pump/probe vibrational lifetimes of Ph_3CN_3 were determined to be 1.76±0.03 ps and 57.62±3.41 ps. Similarly, the parallel polarization measurements yielded lifetimes of 1.7±0.1 ps and 52±3 ps. Both lifetime decays exhibited similar amplitudes of 71.3% and 28.7%.

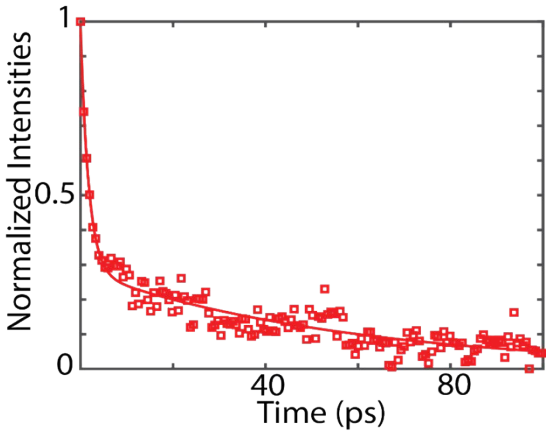

Figure S12. Normalized pump/probe vibrational lifetime decay of Ph_3CN_3 at the magic angle.

Signal-to-noise ratio.

The signal-to-noise (S/N) ratio was calculated from expanding the frequency range of the 2D IR spectrum of $Bu_3Sn^{15}N_3$ in THF, shown in Figure S13. The signal to noise was calculated by measuring the ratio of the 2D IR positive going signal to background signals at different waiting times for different compounds. The S/N ratio at early time (T=1ps) for $Bu_3Sn^{15}N_3$ in THF is 2.6 ± 0.1, an acceptable and reasonable value as shown in prior studies.[14] However, as mentioned above, the S/N ratio of the 2D IR spectrum at later times may decrease significantly allowing the spectrum to become slightly distorted. For example, after observing similar values for the S/N ratio at early times for the 2D IR spectrum of $Ph_3C^{15}N_3$ in THF, the S/N ratio of the spectrum decreases to a value of 0.26 ± 0.03 after a waiting time of 100 ps.

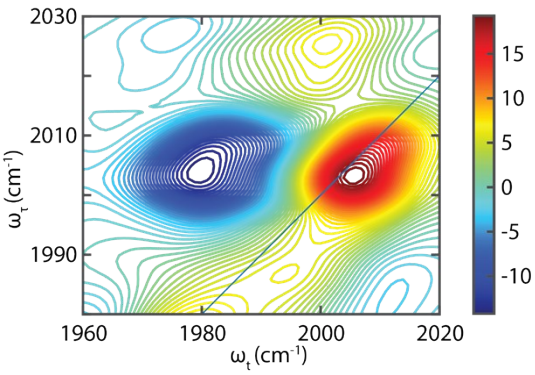

Figure S13. Expanded spectral region of 2D IR spectrum of Figure 4C, $Bu_3Sn^{15}N_3$, in THF at T=2 ps.

Frequency-Frequency correlation decay.

Showing one advantage of the long lifetime azido- probes, the frequency-frequency correlation decay was determined from the spectrum of $Bu_3Sn^{15}N_3$ in THF over a longer time range of 0 to 13 ps. The resulting correlation decay was best fit by a bi-exponential function yielding values of 532 ± 455 fs and 6.9 ± 1.0 ps, shown in Figure S14. The longer component is similar to values observed in literature of probes in THF.[15] However, unlike with some shorter lifetime probes, the longer component (6.9 ± 1.0 ps) can more accurately be captured demonstrating the utility of these probes for studying longer timescale dynamics in biological systems.

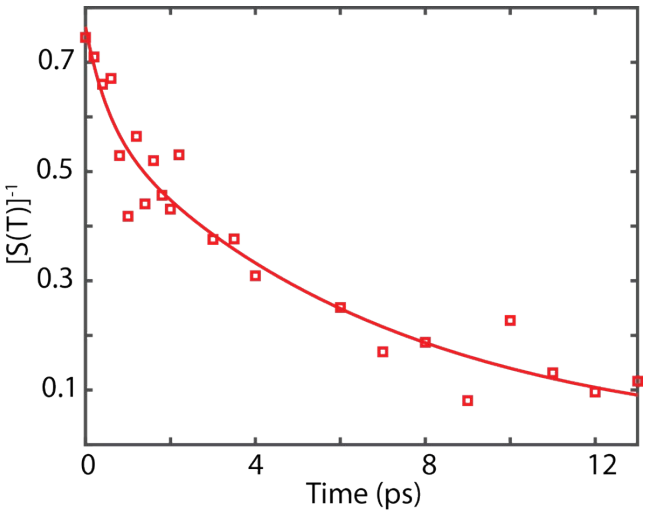

Figure S14. Correlation decay of $Bu_3Sn^{15}N_3$ in THF (red dots) and the bi-exponential fit (red line).

REFERENCES

1. W. H. Saunders and J. C. Ware, *Journal of the American Chemical Society*, 1958, **80**, 3328-3332.
2. A. Kuhn and W. Sander, *Organometallics*, 1998, **17**, 4776-4783.
3. J. S. Thayer and R. West, *Inorganic Chemistry*, 1964, **3**, 406-409.
4. J. G. A. Luijten, G. J. M. Vanderkerk and M. J. Janssen, *Recueil Des Travaux Chimiques Des Pays-Bas-Journal of the Royal Netherlands Chemical Society*, 1962, **81**, 202-205.
5. J. M. Chretien, G. Kerric, F. Zammattio, N. Galland, M. Paris, J. P. Quintard and E. Le Grognec, *Advanced Synthesis & Catalysis*, 2019, **361**, 747-757.

6. K. H. Park, J. Jeon, Y. Park, S. Lee, H. J. Kwon, C. Joo, S. Park, H. Han and M. Cho, *Journal of Physical Chemistry Letters*, 2013, **4**, 2105-2110.
7. Y. S. Kim, J. P. Wang and R. M. Hochstrasser, *Journal of Physical Chemistry B*, 2005, **109**, 7511-7521.
8. M. J. Frisch, G. W. Trucks, H. B. Schlegel, G. E. Scuseria, M. A. Robb, J. R. Cheeseman, G. Scalmani, V. Barone, G. A. Petersson, H. Nakatsuji, X. Li, M. Caricato, A. V. Marenich, J. Bloino, B. G. Janesko, R. Gomperts, B. Mennucci, H. P. Hratchian, J. V. Ortiz, A. F. Izmaylov, J. L. Sonnenberg, Williams, F. Ding, F. Lipparini, F. Egidi, J. Goings, B. Peng, A. Petrone, T. Henderson, D. Ranasinghe, V. G. Zakrzewski, J. Gao, N. Rega, G. Zheng, W. Liang, M. Hada, M. Ehara, K. Toyota, R. Fukuda, J. Hasegawa, M. Ishida, T. Nakajima, Y. Honda, O. Kitao, H. Nakai, T. Vreven, K. Throssell, J. A. Montgomery Jr, J. E. Peralta, F. Ogliaro, M. J. Bearpark, J. J. Heyd, E. N. Brothers, K. N. Kudin, V. N. Staroverov, T. A. Keith, R. Kobayashi, J. Normand, K. Raghavachari, A. P. Rendell, J. C. Burant, S. S. Iyengar, J. Tomasi, M. Cossi, J. M. Millam, M. Klene, C. Adamo, R. Cammi, J. W. Ochterski, R. L. Martin, K. Morokuma, O. Farkas, J. B. Foresman and D. J. Fox, *Journal*, 2016.
9. C. T. Lee, W. T. Yang and R. G. Parr, *Physical Review B*, 1988, **37**, 785-789.
10. A. D. Becke, *Journal of Chemical Physics*, 1993, **98**, 5648-5652.
11. R. Krishnan, J. S. Binkley, R. Seeger and J. A. Pople, *Journal of Chemical Physics*, 1980, **72**, 650-654.
12. A. D. McLean and G. S. Chandler, *Journal of Chemical Physics*, 1980, **72**, 5639-5648.
13. P. J. Hay and W. R. Wadt, *Journal of Chemical Physics*, 1985, **82**, 270-283.
14. S. L. Logunov, V. V. Volkov, M. Braun and M. A. El-Sayed, *Proceedings of the National Academy of Sciences*, 2001, **98**, 8475-8479.
15. M. J. Tucker, X. S. Gai, E. E. Fenlon, S. H. Brewer and R. M. Hochstrasser, *Physical Chemistry Chemical Physics*, 2011, **13**, 2237-2241.